Journal of Physics: Conference Series **420** (2013) 012006 doi:10.1088/1742-6596/420/1/012006

# Coupled-channel study of fine structure in the $\alpha$ decay of $^{233,235}$U

**Dongdong Ni**[1] **and Zhongzhou Ren**[1,2,3]

[1]Department of Physics, Nanjing University, Nanjing 210093, China
[2]Kavli Institute for Theoretical Physics China, Beijing 100190, China
[3]Center of Theoretical Nuclear Physics, National Laboratory of Heavy-Ion Accelerator, Lanzhou 730000, China

E-mail: dongdongnick@gmail.com and zren@nju.edu.cn

**Abstract.** The fine structure observed in the $\alpha$ decay of two deformed uranium isotopes $^{233,235}$U has been investigated by using the coupled-channel Schrödinger equation with outgoing wave boundary conditions. The coupled-channel effect resulting from nuclear deformation is included, and the internal effect of daughter states is considered in dealing with the interaction matrix and the $\alpha$-cluster formation. The experimental branching ratios for various daughter states are well reproduced by the multichannel microscopic calculation. Moreover, the $\alpha$-preformation factor is also discussed by comparison of the calculated half-life with the experimental value.

## 1. Introduction

Alpha decay was observed by Rutherford about a century ago and interpreted as a quantum tunneling effect of preformed $\alpha$ particles independently by Gamow [1] and by Condon and Gurney [2] in 1928. Continual attention has been paid to its importance from both experimental and theoretical sides [3, 4, 5, 6, 7, 8, 9, 10, 11, 12]. An experimental combination of $\alpha$ decay and $\gamma$ emission can greatly help the spectroscopic study of unstable nuclei [13, 14]. This is particularly evident in the experimental study of deformed nuclei owing to the observation of fine structure in $\alpha$ decay. That is, in the deformed system, the low-lying excited states are closely distributed near the ground states so that they are all accessible to $\alpha$ transitions; furthermore, there is significant mixing of these decay channels during the tunneling.

For even-even nuclei, the decay generally proceeds from ground $0^+$ states to various members of the ground-state rotational band (i.e., $0^+$, $2^+$, $4^+$, $6^+$...). Recently the fine structure in even-even $\alpha$ emitters has been investigated using various theoretical models consisting of semiclassical and coupled-channel approaches. The semiclassical methods, based on the one-dimensional Wentzel-Kramers-Brillouin (WKB) approximation, introduce the non-zero angular momentum of $\alpha$ particles and ignore the coupling effect of decay channels. The decay widths for the transitions to various daughter states are separately evaluated at slightly different decay energies and various centrifugal barriers, such as the simple WKB barrier penetration approach [15], generalized liquid drop model (GLDM) [16], unified model for $\alpha$ decay and $\alpha$ capture (UMADAC) [17], and Coulomb and proximity potential model for deformed nuclei (CPPMDN) [18]. In contrast, the coupled-channel methods [19, 20, 21, 22, 23], based on the three-dimensional Schrödinger equation with outgoing wave boundary conditions, take into account

 

the coupling effect and give an active response to the nature of $\alpha$ decay (i.e., three-dimensional quantum tunneling effect). Within the couple-channel framework, we have performed systematic calculations of the fine structure in the $\alpha$ decay of even-even rotational nuclei [22, 23], where two different techniques are used to deal with the coupling interaction matrix. The calculated results show good agreement with the experimental data for both total $\alpha$-decay half-lives and branching ratios for various daughter states.

The objective of this article is to extend our coupled-channel study from even-even nuclei to odd-mass nuclei. In contrast to the $\alpha$ decay of even-even nuclei, the situation for the case of odd-$A$ emitters is much more complicated owing to the last unpaired nucleon. Besides the increasing rotational bands in the daughter nuclei, the number of partial waves that are required in the decomposition of the total wave function increases greatly. For example, there is one single channel $\ell = J_d$ for the $\alpha$ transition $0^+ \rightarrow J_d$ in even-even nuclei, while the $\alpha$ transition $J \rightarrow J_d$ in odd-$A$ nuclei allows several channels with $|J - J_d| \leq \ell \leq (J + J_d)$. As we all know, including one more channel in the coupled-channel study would require considerable increase in numerical stability and computation time. Just for this difficulty, there has been no coupled-channel calculation of the $\alpha$-decay fine structure observed in odd-$A$ nuclei. In this work, the theoretical attempt is made to describe the fine structure in the $\alpha$ decay of $^{233,235}$U. As shown below, the available experimental data concerning $\alpha$-decay half-lives and branching ratios for various daughter states can be well reproduced in a straightforward and consistent manner.

## 2. Theoretical framework for deformed $\alpha$ decays

The total wave function of the decaying system with a particular total spin ($JM$) can be expanded into a sum of partial waves with angular and radial components:

$$\Psi_{JM} = \phi(\alpha) r^{-1} \sum_{I\ell} u^J_{n\ell I}(r) [Y_\ell(\hat{\mathbf{r}}) \otimes \Phi_I]_{JM}. \tag{1}$$

where $\phi(\alpha)$ is the internal wave function of the $\alpha$ particle, $u^J_\alpha$ [$\alpha \equiv (n\ell I)$ labels the channel quantum numbers] is the cluster radial function, $Y_\ell(\hat{\mathbf{r}})$ is the orbital wave function of the $\alpha$ particle, and $\Phi_I$ is the wave function of the daughter nucleus characterizing the rotation of the core with excitation energies, $H_d \Phi_I = E_I \Phi_I$.

After inserting (1) into the Schrödinger equation and projecting the equation onto the angular part, one obtains the coupled-channel equations for the radial components

$$\Big[ -\frac{\hbar^2}{2\mu}\Big(\frac{d^2}{dr^2} - \frac{\ell_\alpha(\ell_\alpha+1)}{r^2}\Big) - (Q_0 - E_I)\Big] u_\alpha(r) + \sum_{\alpha'} V_{\alpha,\alpha'}(r) u_{\alpha'}(r) = 0. \tag{2}$$

In this equation, $Q_0$ is the $Q_\alpha$ value for the decay to the daughter ground state, and the quantity $V_{\alpha,\alpha'}(r)$ is the matrix element of the interaction $V$ taken between channels $\alpha$ and $\alpha'$. The deformed potential $V$ consists of the attractive nuclear and repulsive Coulomb parts. The nuclear potential between the $\alpha$ cluster and the deformed core nucleus has a simple axially deformed Woods-Saxon (WS) form [23]. The Coulomb potential of the $\alpha$ cluster with the core is approximated to the first order in $\sum_\ell \beta_\lambda Y_{\lambda 0}(\theta)$ [22, 24].

The interaction matrix elements are obtained by making a multipole expansion of the potential $V$ [19, 20, 21, 23], $V = \sum_{\lambda=0}^{\lambda_{\max}} \upsilon_\lambda(r)(\Omega_\lambda \otimes Y_\lambda)_{00}$, where only even values of $\lambda$ appear in the summation owing to the axial symmetry. It is then convenient to evaluate the matrix element of $V$ in terms of the angular momentum theory [23, 25, 26]:

$$V_{\alpha,\alpha'}(r) = \sum_\lambda \upsilon_\lambda(r) \langle \Phi_I \| \Omega_\lambda \| \Phi_{I'} \rangle \times A(\ell I, \ell' I', \lambda J), \tag{3}$$

where the factor $A$ is purely geometric and comes from the proper coupling of angular momentum vectors. The reduced matrix elements of $\Omega_\lambda$ contain all of the dynamics of the daughter core. For rotational nuclei, they are assumed of the form [23, 25, 26],

$$\langle \Phi_I \| \Omega_\lambda \| \Phi_{I'} \rangle = \sqrt{\frac{(2\lambda+1)(2I'+1)}{4\pi(2I+1)}} \langle I'\lambda K0 | IK \rangle, \tag{4}$$

where $\langle ab\alpha\beta | c\gamma \rangle$ is the Clebsch-Gordan coefficient and $K$ is the angular momentum projection on the symmetry axis ($K = 0$ for even-even nuclei). The off-diagonal coupling appears due to the non-spherical parts of WS and Coulomb potentials. Here, the WS potential is decomposed into spherical multipoles to order 12, which is sufficient for good stability [23].

The coupled equations (2) are solved with the following boundary conditions. First, the channel wave functions are regular at the origin, $u_{n\ell I}(r \to 0) \to 0$. Second, in the asymptotic region the nuclear potential vanishes and the Coulomb potential is spherically symmetric. At this point the coupled-channel equations decouple, and the channel wave functions behave as outgoing Coulomb-Hankel waves, $u_{n\ell I}(r) \sim G_\ell(k_I r) + iF_\ell(k_I r)$ with $k_I = \sqrt{2\mu(Q_0 - E_I)}/\hbar$. Moreover, the eigencharacteristic of each solution should follow the Wildermuth rule [27], $G = 2n + \ell = \sum_{i=1}^{4} g_i$, where $g_i$ are the corresponding oscillator quantum numbers of the constituent nucleons in the $\alpha$ cluster. In fact, the situation of single-particle states is much more complicated especially for deformed nuclei. So the rule is only an approximation treatment of the Pauli exclusion principle, but it remains useful as a guide for setting the global quantum number $G$. Here, the $G$ number is fixed at $G = 22$ for U isotopes.

During the solution of the equations (2), the depth of the WS potential is adjusted so as to make all channels simultaneously reproduce the experimental $Q_I$ values and satisfy the Wildermuth rule. Ultimately, one can express the partial width of the channel $\ell I$ as [22, 23]

$$\Gamma_{\ell I}(R) = \frac{\hbar^2 k_I}{\mu} \frac{|u_{n\ell I}(R)|^2}{G_\ell(k_I R)^2 + F_\ell(k_I R)^2}, \tag{5}$$

where $R$ denotes large distances beyond the range of the nuclear potential and beyond the distance where the Coulomb potential can be regarded as spherically symmetric. It should be particularly noted that the expression of $\Gamma_{\ell I}(R)$ is rather insensitive to the choice of $R$.

Next, the structure part of $\alpha$ decay can be evaluated by using a constant $\alpha$-preformation factor $P_\alpha$ together with the hypothesis of the Boltzmann distribution (BD) for daughter states, $\rho(E_I) = \exp(-cE_I)$ [21, 23]. The procedure proposed is based on the available experimental facts and theoretical analysis [28, 29, 30, 31, 32, 33]. And it has been proven to be successful in describing the fine structure in the $\alpha$ decay of even-even nuclei [22, 23]. In combination with the evaluation of the partial decay width, the total width is given by $\Gamma = \sum_{\ell I} P_\alpha \rho(E_I) \Gamma_{\ell I}(R)$, and then the half-life for alpha decay is $T_{1/2} = \hbar \ln 2/\Gamma$.

## 3. Numerical results and discussion

Using the formalism described above, we have performed a detailed investigation on the fine structure in the $\alpha$ decay of $^{233,235}$U. These two emitters are at the gateway to the well-deformed heavy nuclei region, and the excitation spectrums of their daughter nuclei exhibit strong collective rotational motion. Moreover, the experimental measurements of the $\alpha$-decay fine structure for $^{233,235}$U are relatively full [34]. The coupled-channel study of these two nuclei not only affords us an excellent opportunity to test the developed $\alpha$-decay model but also lay the groundwork for further extensions towards odd-$A$ $\alpha$ emitters with large deformations.

Special attention should be paid to make sure that enough decay channels are included in the coupled-channel calculations. The previous coupled-channel study of even-even nuclei has shown

**Table 1.** Main input information needed in the calculations, including the decay energy, spin-parity of the decaying state, deformation parameters of the daughter nucleus, band head of the major daughter rotational bands, together with the excitation energies of the two lowest-lying members.

| Emitter | $Q_0$ (MeV) | $J^\pi$ | $\beta_2$ | $\beta_4$ | $K^\pi$ | $E_K$ (keV) | $E_{K+1}$ (keV) |
|---|---|---|---|---|---|---|---|
| $^{233}$U | 4.9085 | $5/2^+$ | 0.190 | 0.114 | $5/2^+$ | 0.0 | 42.4349 |
| $^{235}$U | 4.6787 | $7/2^-$ | 0.198 | 0.115 | $5/2^-$ | 185.714 | 205.309 |
| | | | | | $7/2^-$ | 387.827 | 452.18 |

that including all partial waves with $\ell \leq 8$ is enough for proper convergence [23]. Therefore, following [23], all decay channels with $\ell \leq 8$ are taken into account in the calculations. The number of decay channels depends on the spin-parity $J^\pi$ of the decaying state and the band head $K^\pi$ of the final rotational band. For example, the $\alpha$ decay from ground $5/2^+$ states to $K = 5/2^+$ rotational bands exhibits 21 decay channels. The $\alpha$ decay from ground $7/2^-$ states to $K = 7/2^-$ rotational bands exhibits 24 decay channels.

In our calculations, the experimental data of $\alpha$-decay half-lives, branching ratios, and rotational spectrums are taken from the NuDat database [34] and the deformation parameters of the daughter nuclei are set by the theoretical calculations of Möller *et al.* [35]. In some cases, the data on high excitation spectrum $E_I$ are absent in experiments. For this, we use the first-order perturbation theory [36]: for a $K = 1/2$ band

$$E_I = E_{1/2} + \frac{1}{2\Im}\Big[I(I+1) - 3/4 + a + a(-)^{I+1/2}(I+1/2)\Big], \tag{6}$$

and for a $K \neq 1/2$ band

$$E_I = E_K + \frac{1}{2\Im}\Big[I(I+1) - K(K+1)\Big], \tag{7}$$

where $\Im$ and $a$ are the parameters to be determined from the known low-lying excitation energies. Table 1 displays the main input information for the two nuclei under investigation. The second column is the decay energy $Q_0$ for the transition to ground states. The third column denotes the spin-parity $J^\pi$ of the decaying state. Columns 4 and 5 give the deformation $\beta_2$ and $\beta_4$ parameters of the daughter nucleus. Column 6 lists the band head $K^\pi$ of the main daughter rotational bands involving in $\alpha$ transitions, and the excitation energies $E_K$ and $E_{K+1}$ of the two lowest-lying members of the rotational bands are shown in the last two columns. To avoid introducing additional parameters into the calculation, we use the same parameters as in the previous study of even-even $\alpha$ emitters [23] except for the $\alpha$-preformation factor $P_\alpha$.

First, we restrict our attention on one kind of interesting $\alpha$ transitions, where the band head of the daughter rotational band is the same as the spin-parity of the decaying state, i.e., $K^\pi = J^\pi$. Figure 1 shows the numerical results of the calculated branching ratios (BRs). Note that the calculated BRs are normalized for comparison with the available experimental data; that is to say, the sum of the calculated BRs equals to that of the experimental data. As one can see, there are clear differences in the BRs between the two emitters: the BRs for the $K^\pi = J^\pi$ transitions take a significant place in the $\alpha$ decay of $^{233}$U, while the $K^\pi = J^\pi$ transitions have a weak contribution to the $\alpha$ decay of $^{235}$U [34]. This could be attributed to the location of the $K^\pi = J^\pi$ rotational band: in the former case the $K^\pi = J^\pi = 5/2^+$ band belongs to ground-state rotational bands, while in the latter case the $K^\pi = J^\pi = 7/2^-$ band locates in the highly excited region where the $\alpha$ transitions are hindered to some extent owing to the relatively small

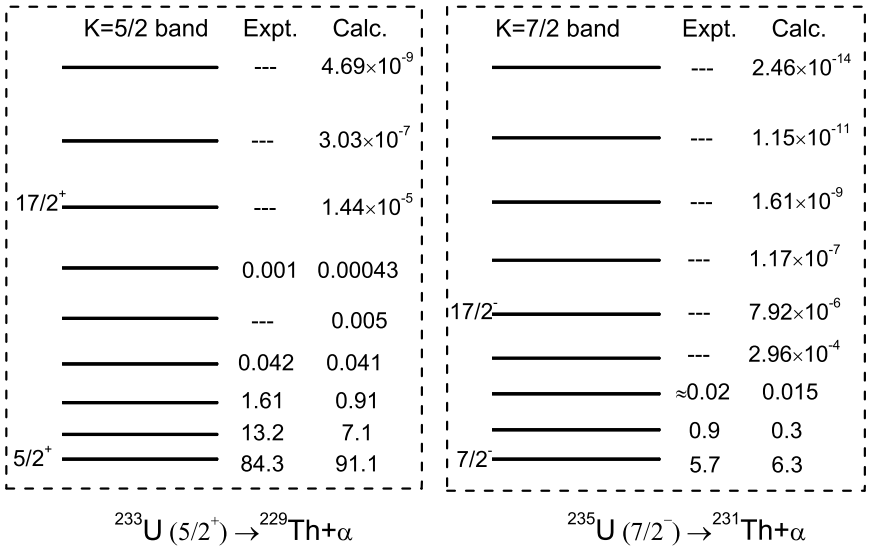


**Figure 1.** Comparison of the calculated branching ratios (in %) with the available experimental data for the $\alpha$ transitions from the ground $J^\pi$ state to the $K^\pi = J^\pi$ rotational band in $^{233,235}$U.

$Q_\alpha$ values. In spite of these differences, the theoretical values of the BRs follow the experimental ones well over a range of magnitude, from 0.001% to 100%. Besides, without inclusion of the preformation factor (i.e., $P_\alpha = 1$), the calculated $\alpha$-decay half-lives $T_{\rm calc.}$ for $^{233,235}$U are obtained as $2.52\times10^{12}$ s and $8.48\times10^{16}$ s, respectively. Experimentally, the measured half-lives $T_{\rm expt.}$ for them are known as $5.07\times10^{12}$ s and $3.35\times10^{17}$ s [34]. The ratios $T_{\rm calc.}/T_{\rm expt.}$ between the calculated results and the experimental data suggest the preformation factor $P_\alpha$ within the range of 0.2−0.4. This is quite consistent with the analysis of favored $\alpha$ transitions in odd-$A$ nuclei [37, 38]. The explicit determination of the $P_\alpha$ value needs systematic $\alpha$-decay calculations of a wide range of deformed odd-$A$ nuclei. This is worth us further investigation in the near future.

As has been mentioned above, the $\alpha$ transitions from the ground $7/2^-$ state to the $K^\pi = 7/2^-$ rotational band play a minor role in the $\alpha$ decay of $^{235}$U. By contrast, the transitions to the $K^\pi = 5/2^-$ rotational band play a major role [34]. Next, we shall perform a detailed study of such $\alpha$ transitions. The comparison of the calculated BRs with the available experimental data is shown in figure 2. It is seen from figure 2 that the calculated BRs agree well with the experimental data. The largest deviation of our analysis in the figure emerges at the transition $7/2^- \to 5/2^-$, for which the BR is predicted as 12.6% but the experimental value is known as 2.1% [34]. New measurements of this BR with high precision would be most welcome to test the validity of the calculations of this study. In addition, the comparison of the calculated $\alpha$-decay half-life $T_{\rm calc.} = 2.76 \times 10^{15}$ s with the experimental value $T_{\rm expt.} = 2.81 \times 10^{16}$ s evaluates the preformation factor as $P_\alpha = T_{\rm calc.}/T_{\rm expt.} \approx 0.10$. This value is more than two times smaller than the previously obtained value 0.2−0.4. The reason for this is that the $\alpha$-cluster formation in the former case only involves paired nucleons without the change of the last unpaired nucleon, similar to $\alpha$ decays in even-even nuclei, while the cluster formation studied here involves unpaired nucleons, leading to considerable hindrance [37]. In spite of the good agreement between experiment and theory shown in figure 1 and figure 2, the coupled-channel

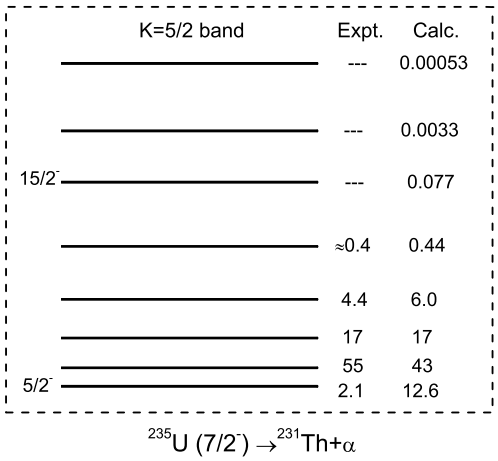


**Figure 2.** Same as in figure 1, but for the $\alpha$ transitions from the ground $7/2^-$ state to the $K^\pi = 5/2^-$ rotational band in $^{235}$U, which are more preferred with respect to the transitions to the $K^\pi = 7/2^-$ band.

study of the $\alpha$ decay of $^{233,235}$U is merely the beginning because the actual situation of $\alpha$ transitions in deformed odd-$A$ nuclei may be much more complex than what we expect. It is interesting and desired to further use reliable nuclear structure models to achieve a complete description of the fine structure observed in the $\alpha$ decay of odd-$A$ nuclei.

## 4. Summary

In summary, we have presented in this paper a detailed study of the fine structure in the $\alpha$ decay of deformed $^{233,235}$U. The decay widths are calculated by solving the coupled-channel Schrödinger equation with outgoing wave boundary conditions, instead of using the simple semiclassical WKB method. The $\alpha$-cluster formation is considered by using the constant preformation factor in combination with the BD hypothesis of daughter states. Or in other words, the internal effect of daughter states on the $\alpha$-cluster formation is clearly included. For the $\alpha$ transitions from the ground state to the low-lying members of the rotational band, the calculated branching ratios are found to agree well with the available experimental data. And the branching ratios for the transitions to the high-lying members are predicted. In addition, the $\alpha$-preformation factor is also analyzed by comparison of the calculated $\alpha$-decay half-lives with the experimental value. The deduced results are consistent with the other theoretical studies. Despite this, a complete and microscopic description of $\alpha$-particle formation need to be made. This is worth further investigation.

## Acknowledgments

This work is supported by the National Natural Science Foundation of China (Grants No. 10735010, No. 10975072, No. 11035001, and No. 11120101005), by the 973 National Major State Basic Research and Development of China (Grants No. 2007CB815004 and No. 2010CB327803), by CAS Knowledge Innovation Project No. KJCX2-SW-N02, by Research Fund of Doctoral Point (RFDP), Grants No. 20100091110028, and by a Project Funded by the Priority Academic Program Development of Jiangsu Higher Education Institutions (PAPD).

## References

[1] Gamow G 1928 *Z. Phys.* **51** 204
[2] Condon E U and Gurney R W 1928 *Nature* **122** 439
[3] Buck B, Merchant A C, and Perez S M 1993 *At. Data Nucl. Data Tables* **54** 53
[4] Royer G 2000 *J. Phys. G* **26** 1149
[5] Poenaru D N, Plonski I H, and Greiner W 2006 *Phys. Rev.* C **74** 014312
[6] Xu C and Ren Z 2006 *Phys. Rev.* C **73** 041301(R) Xu C and Ren Z 2006 *Phys. Rev.* C **74** 014304
[7] Denisov V Yu and Ikezoe H 2005 *Phys. Rev.* C **72** 064613
[8] Mohr P 2006 *Phys. Rev.* C **73** 031301(R)
[9] Pei J C, Xu F R, Lin Z J and Zhao E G 2007 *Phys. Rev.* C **76** 044326
[10] Kelkar N G and Castañeda H M 2007 *Phys. Rev.* C **76** 064605
[11] Chowdhury P R, Samanta C and Basu D N 2008 *Phys. Rev.* C **77** 044603
[12] Ni D and Ren Z 2009 *Nucl. Phys.* A **825** 145 Ni D and Ren Z 2009 *Nucl. Phys.* A **828** 348
[13] Kettunen H, Uusitalo J, Leino M *et al* 2001 *Phys. Rev.* C **63** 044315
[14] Andreyev A N, Antalic S, Achermann D *et al* 2009 *Phys. Rev.* C **80** 024302
[15] Xu C and Ren Z 2006 *Nucl. Phys.* A **778** 1
[16] Wang Y Z, Zhang H F, Dong J M, and Royer G 2009 *Phys. Rev.* C **79** 014316
[17] Denisov V Yu and Khudenko A A 2009 *Phys. Rev.* C **80** 034603
[18] Santhosh K P, Sahadevan S, and Joseph J G 2011 *Nucl. Phys.* A **850** 34
[19] Delion D S, Peltonen S, and Suhonen J 2006 *Phys. Rev.* C **73** 014315
[20] Peltonen S, Delion D S, and Suhonen J 2008 *Phys. Rev.* C **78** 034608
[21] Ni D and Ren Z 2009 *Phys. Rev.* C **80** 051303(R) Ni D and Ren Z 2010 *Phys. Rev.* C **81** 024315
[22] Ni D and Ren Z 2010 *Phys. Rev.* C **81** 064318
[23] Ni D and Ren Z 2011 *Phys. Rev.* C **83** 067302
[24] Hagino K, Rowley N, and Kruppa A T 1999 *Comput. Phys. Comm.* **123** 143
[25] Kruppa A T, Barmore B, Nazarewicz W, and Vertse T 2000 *Phys. Rev. Lett.* **84** 4549 Barmore B, Kruppa A T, Nazarewicz W, and Vertse T 2000 *Phys. Rev.* C **62** 054315
[26] Suzuki Y and Ohkubo S 2010 *Phys. Rev.* C **82** 041303(R)
[27] Wildermuth K and Tang Y C 1997 *A Unified Theory of the Nucleus* (New York: Academic Press)
[28] Hodgson P E and Běták E 2003 *Phys. Rep.* **374** 1
[29] Lovas R G, Liotta R J, Insolia A, Varga K and Delion D S 1998 *Phys. Rep.* **294** 265
[30] Iriondo M, Jerrestam D, and Liotta R J 1986 *Nucl. Phys.* A **454** 252
[31] Einstein A 1917 *Phys. Z* **18** 121
[32] Stewart T L, Kermode M W, Beachey D J *et al* 1996 *Phys. Rev. Lett.* **77** 36
[33] Delion D S 2009 *Phys. Rev.* C **80** 024310
[34] NNDC of the Brookhaven National Laboratory, http://www.nndc.bnl.gov.
[35] Möller P, Nix J R, Myers W D, and Swiatecki W J 1995 *At. Data Nucl. Data Tables* **59** 185
[36] Bohr A and Mottelson B R 1998 *Nuclear Structure Vol. 1* (World Scientific, Singapore)
[37] Ni D and Ren Z 2009 *Phys. Rev.* C **80** 014314
[38] Ni D and Ren Z 2010 *J. Phys. G: Nucl. Part. Phys.* **37** 035104